Predicting Lead Vehicle Velocity for Eco-Driving in the Absence of V2V Information

2023-01-0220

Predicting Lead Vehicle Velocity for Eco-Driving in the Absence of V2V Information

Vinith Kumar Lakshmanan[1], Shobhit Gupta[2], Stefano D'Alessandro[2], Matteo Spano[2], Dennis Kibalama[2], Stephanie Stockar[2], Marcello Canova[2], Ouafae El Ganaoul-Mourlan[1], Antonio Sciarretta[1]

[1]IFP Energies Nouvelles, [2]The Ohio State University

Abstract

Accurately predicting the future behavior of the surrounding traffic, especially the velocity of the lead vehicle is important for optimizing the energy consumption and improve the safety of Connected and Automated Vehicles (CAVs). Several studies report methods to predict short-to-mid-length lead vehicle velocity using stochastic models or other data-driven techniques, which require availability of extensive data and/or Vehicle-to-Vehicle (V2V) communication. In the absence of connectivity, or in data-restricted cases, the prediction must rely only on the measured position and relative velocity of the lead vehicle at the current time. This paper proposes two velocity predictors to predict short-to-mid-length lead vehicle velocity. The first predictor is based on a Constant Acceleration (CA) with an augmented stop mode. The second one is based on a modified Enhanced Driver Model (EDM-LOS) with line-of-sight feature. Both predictors rely only on information on the present values of lead vehicle position and velocity to compute a future velocity estimate. An analysis is done to compare the prediction accuracy of the proposed predictors with different experimental driving data recorded using an OBD2 scanner plugged into a passenger vehicle. Finally, the predicted lead vehicle velocity is utilized to formulate time-gap constraints for the eco-driving optimal control problem, solved via Model Predictive Control (MPC). The energy savings of the considered velocity predictors are evaluated by performing a large-scale simulation study. The proposed velocity predictor provides closest energy savings to a wait-and-see solution for a CAV in absence of V2V communication.

Introduction

Advancements in navigation systems and Vehicle-to-Everything (V2X) communication have led to the access of a wealth of information from the environment and infrastructure, such as traffic density, location and velocity of surrounding vehicles, upcoming road topology, grade, speed limits, etc. Connected and automated vehicles (CAVs) can access such information to improve the safety and comfort. In recent times, control strategies have been developed that leverage the look-ahead information available to CAVs to save energy, often referred to as eco-driving [1,2,3,4,5]. Despite the energy efficiency improvements and other benefits demonstrated by these technologies, uncertainties in the traffic environment can limit the ability of eco-driving controllers to smoothen the velocity profile and might eventually lead to decline in energy savings [6]. For real-time implementation of eco-driving controllers with consistent energy savings, it becomes necessary to include the dynamics of the traffic, especially the estimated future lead vehicle velocity into the eco-driving's trajectory planning process. Fig. 1 describes an example of an eco-driving controller that integrates the signal phase and timing information from vehicle-to-infrastructure (V2I) communication and lead vehicle velocity prediction from vehicle-to-vehicle (V2V) communication into a short-term trajectory optimization framework. Lead vehicle here refers to the immediately preceding vehicle to the ego vehicle that can cause a potential rear-end collision. Predicting the speed trajectory of a lead vehicle plays a vital role in improving the safety and energy consumption of CAVs. In fact, inaccurate prediction of the lead vehicle speed may lead to an overreaction of the ego CAV, causing unwanted accelerations/decelerations and ultimately worse energy consumption than a purely reactive control strategy [6,7].

Predicting a vehicle's speed is highly dependent on the amount of information on that vehicle and its surroundings, and the used prediction method. A comprehensive overview of the existing prediction methods can be found in [8]. The ego CAV can obtain information on the lead vehicle and its surroundings using either sensors and/or V2X communication, as shown in Fig. 1. The methods found in the literature for predicting speed trajectories can be broadly classified as data-driven or model-based.

Data-driven time-series prediction methods such as long-short-term memory [1,12], or gated recurrent network [13], have been extensively used to perform mid-long length speed predictions. However, these methods require the availability of extensive training data and/or V2V communication.

Model-based approaches include simple models such as constant velocity and Constant Acceleration (CA). The constant velocity predicts the lead vehicle to maintain the current speed over the future prediction horizon while the CA assumes the vehicles' future speed to move with the same acceleration until it stops or exceeds a maximum velocity. However, these models lack adaptability to variations in driving styles and in certain cases are unrealistic. More sophisticated microscopic car-following models such as the Intelligent Driver Model [9], the Line-Of-Sight-based Enhanced Driver Model (EDM-LOS) [10], or Gipps' model [11], which are in principle used to model driver behavior, could also be used to predict the lead vehicle's velocity. Such microscopic models include parameters for driving style calibration, allowing to capture various driver behaviors. While model-based methods loose accuracy over long term prediction, they perform reasonably well in short term horizon, which is the main focus of this paper.

This paper presents a comparison of two methods to predict the lead vehicle velocity over a short-term horizon in the absence of connectivity (V2V/V2X) or under data-restricted cases. In such scenarios, the prediction must rely only on the measured position and relative velocity of the lead vehicle at the current time. Two methods are considered in this study, namely, a Constant Acceleration (CA) model and a Line-of-Sight based Enhanced Driver Model (EDM-LOS). The CA uses the current detected velocity and acceleration of the lead vehicle to predict the future velocity for short instances of time. However, when approaching a fixed obstacle such as a traffic light or intersection, the CA model prediction may become inaccurate, resulting in the inability to correctly stop the ego vehicle at the intersection. The EDM-LOS model without the information about the vehicle preceding the lead vehicle fails to predict braking events during car-following.

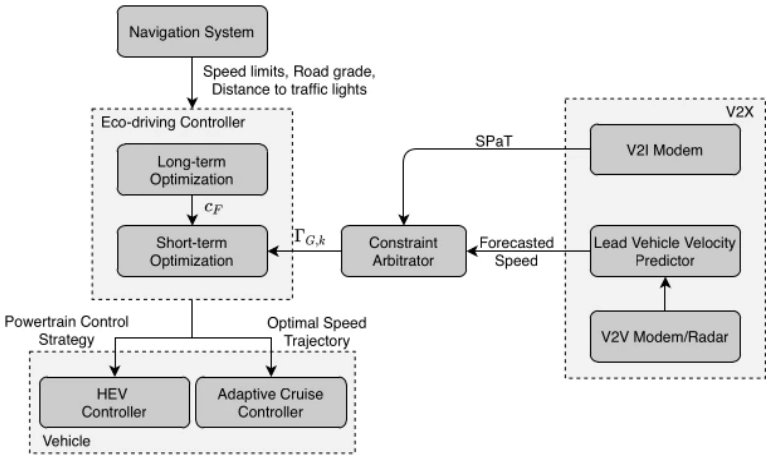

Figure 1. Hierarchical eco-driving control architecture leveraging V2X technology in presence of lead vehicle.

The contributions of this work are as follows. Two lead vehicle velocity predictors are developed, namely Constant Acceleration-Average Braking (CA-AB) and EDM-LOS based Predictor (EDM-LOSP). The CA-AB is an improved model over CA in predicting decelerations to a stop in the presence of an obstacle. The EDM-LOSP is an improved model over EDM-LOS to identify and predict braking events during car-following. The performance of the proposed predictors is evaluated for energy efficiency and travel time in a simulation-based environment using real-world driving profiles and compared against CA as baseline and an ideal scenario with perfect velocity prediction (wait-and-see) as benchmark.

The paper is organized with the following section describing the vehicle model, formulation of the optimal control problem and the lead vehicle constraint. The section after, describes the methods for predicting the lead vehicle's trajectory and the following section discusses the evaluation of the predictors in a simulation environment along with its results. Concluding remarks are provided in the final section.

Vehicle Model and Problem Formulation

This section describes the mild hybrid vehicle model considered in this study and the eco-driving optimal control problem formulation.

Mild Hybrid Electric Vehicle Model

A forward-looking model of a P0 parallel mild-hybrid vehicle is adopted in this work to predict the longitudinal dynamics and energy consumption, as shown in Fig. 2 [14]. A Belted Starter Generator (BSG) is connected to a 1.8 L turbocharged gasoline engine and a 48V battery pack. The inputs to the model are obtained from a simplified electronic control module (ECM) that contains a production level torque split strategy and converts the driver's pedal position to desired engine torque T_{eng}^{des} and desired BSG torque T_{bsg}^{des}. The vehicle simulator contains a low-frequency powertrain and longitudinal vehicle dynamics model, as well as quasi-static models of engine (fuel maps), BSG (torque limit and efficiency maps), torque converter and transmission. Model validation was performed in a previous study [14] on a chassis dynamometer over the FTP cycle. Despite few mismatches in the state of charge, the error on the predicted fuel consumption is less than 4%, which can be considered sufficiently accurate for this work.

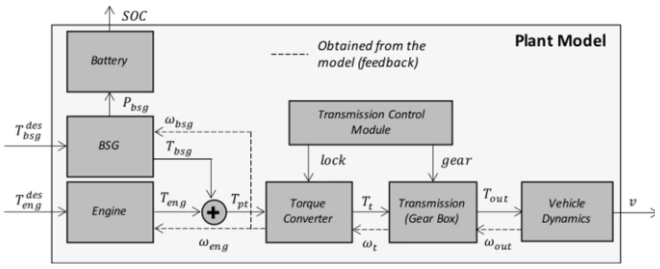

Figure 2. Qualitative schematics of a 48 V mild hybrid electric drivetrain.

Optimal Control Problem

The eco-driving control problem is formulated as a non-linear optimal control problem in spatial domain, aimed at minimizing a trade-off between fuel consumption and travel time over an itinerary of N steps. In this work, the state variables chosen are the vehicle velocity, battery state of charge (SoC) and travel time: $x_s = [v_s, \xi_s, t_s]^T \in \mathcal{X} \subset \mathbb{R}^n$. The engine torque and BSG torque are chosen as the control variables: $u_s = [T_{engs}, T_{bsg,s}]^T \in \mathcal{U} \subset \mathbb{R}^m$. Note that all predictions are denoted using $\widehat{(.)}$ and observed/measured signals are denoted using $(.)_0$.

Consider a dynamic control problem discretized in the spatial domain with the form:

$$x_{s+1} = f(x_s, u_s), \qquad s = 1, \dots, N \tag{1}$$

where s is the discrete position, and f is a function that describes the state dynamics and is derived in [13]. The admissible control maps at position s is denoted by $\mu_s: \mathcal{X} \to \mathcal{U}$, which satisfies the constraint function $h_s: \mathcal{X} \times \mathcal{U} \to \mathbb{R}^r$, expressed as $h(x_s, u_s) \leq 0, \forall, x \in \mathcal{X}$:

$$v_s \in [v_s^{min}, v_s^{max}], \qquad \forall s = 1, \dots, N \tag{2a}$$

$$\xi_s \in \left[\xi_s^{min}, \xi_s^{max}\right], \qquad \forall s = 1, \dots, N \tag{2b}$$

$$t_s \in [0, t_N], \qquad \forall s = 1, \dots, N \tag{2c}$$

$$v_0 = v_0^{min}, \qquad \xi_0 \in [\xi^{min}, \xi^{max}] \tag{2d}$$

$$a_s \in \left[a^{min}, a^{max}\right], \qquad \forall s = 1, \dots, N \tag{2e}$$

$$T_{eng,s} \in \left[T_{eng,s}^{min}, T_{eng,s}^{max}\right], \qquad \forall s = 0, \dots, N \tag{2f}$$

$$T_{bsg,s} \in \left[T_{bsg,s}^{min}, T_{bsg,s}^{max}\right], \qquad \forall s = 0, \dots, N \tag{2g}$$

where v_s^{min}, v_s^{max} refer to the minimum and maximum speed limit; ξ_s^{min}, ξ_s^{max} refer to the minimum and maximum SoC limits; a^{min}, a^{max} refer to the vehicle acceleration for comfort; $T_{eng,s}^{min}, T_{eng,s}^{max}$ refer to the engine torque limits; $T_{bsg,s}^{min}, T_{bsg,s}^{max}$ refer to the BSG torque limits respectively. t_N refers to the maximum travel time limit imposed at the end of the route which can be estimated using the time taken to complete the historical trips. To ensure charge-sustenance, $\xi_0 = \xi_N$.

The collection of admissible maps is referred as the policy of the controller, denoted by $\mathcal{M} := \{\mu_0, \dots, \mu_N\}$. The controller minimizes a cost functional over N steps:

$$\min_{\mathcal{M}} \; c_N(x_N) + \sum_{s=0}^{N-1} + c(x_s, \mu_s(x_s)) \tag{3}$$

where $c: \mathcal{X} \times \mathcal{U} \to \mathbb{R}$ is the per-stage cost, defined as the weighted average of fuel consumption and travel time:

$$c(x_s, \mu_s(x_s)) = \left(\gamma \frac{\dot{m}_{f,s}(x_s, \mu_s(x_s))}{\dot{m}_{f,norm}} + (1 - \gamma)\right) t_s \tag{4}$$

where γ is the trade-off, $\dot{m}_{f,s}$ is the fuel flow rate, $\dot{m}_{f,norm}$ is the normalizing factor, and $t_s := \frac{d_s}{\bar{v}_s}$ is the travel time per step. To account for the variability in route conditions such as time-varying signal phase and timing (SPaT) information, the eco-driving problem in Eq. (3) is formulated for $s = 1, \dots, N_{N_H} - 1$, as a receding horizon optimal control problem (RHOCP), minimizing the cost functional over a reduced horizon N_H steps ($\ll N$) [14]:

$$\min_{\mathcal{M}_s} \; c_{s+N_H}\left(x_{s+N_H}\right) + \sum_{k=s}^{s+N_H-1} + c(x_k, \mu_k(x_k)) \tag{5}$$

where N_H is the number of steps in the prediction horizon. In this work, at a position s, it is assumed that the lead vehicle acceleration $\hat{a}_k$ is predicted (as described in the following section) and can be used to predict the lead vehicle velocity $\hat{v}_k^l$ and arrival time $\hat{t}_k^l$ for $k = s, \dots, s + N_{N_H} - 1$, with a step size Δd_k as:

$$\hat{v}_{k+1}^l = \sqrt{(\hat{v}_k^l)^{\,2} + 2\hat{a}_k \Delta d_k} \tag{6a}$$

$$\hat{t}_{k+1}^l = \hat{t}_k^l + \frac{2\Delta d_k}{\hat{v}_k^l + \hat{v}_{k+1}^l} \tag{6b}$$

It should be noted that the constraints (2a), (2b), (2e), (2f) and (2g) remain the same in the RHOCP $\forall s = 1, \dots, N - N_H,\ \forall k = s, \dots, s + N_H$. However, the constraint on the time is affected by imposing time-gap constraint between the ego and lead vehicle as:

$$t_k \geq \hat{t}_k^l + t_{gap} \tag{7}$$

where t_{gap} represents the safety gap to the leader in time.

To include V2I information, additional constraints are imposed on the time such that it lies in the feasible set of travel time for passing-at-green at signalized intersection, $t_k \in \Gamma_{G,k}$ [15].

The RHOCP (5) is solved using Approximate Dynamic Programming (ADP), such that terminal cost of the RHOCP (named "short-term optimization" in Fig. 1) is approximated from the offline solution of a full-route optimization (named "long-term optimization" in Fig. 1) under partial route information [14].

Predicting Lead Vehicle Velocity

The two models considered in this work to predict the lead vehicle velocity within the RHOCP are the CA-AB and the EDM-LOSP. These models are a result of significant improvements made to the CA and EDM proposed in literature [2,3,10]. This section describes the CA and EDM-LOS models, their drawbacks, and the improvements made leading to the CA-AB and EDM-LOSP.

Constant Acceleration – Average Braking (CA-AB)

The CA model predicts the future velocity of the lead vehicle to have a constant acceleration until it reaches the speed limit [17]:

$$\hat{a}^l{}_k = \begin{cases} a_0, & \hat{v}_k^l < v_{lim} \\ 0, & \hat{v}_k^l \geq v_{lim} \ \vee \ \hat{v}_k^l = 0 \end{cases} \tag{8}$$

where a_0 represents the acceleration of the lead vehicle at $k = 0$ (also current time). $\hat{a}^l{}_k$ represents the predicted acceleration. The speed limit of the route is given by v_{lim}. However, when approaching an obstacle such as a traffic light or a stop sign, the CA model is unable to correctly predict where the lead vehicle will be stopping, resulting in the lead vehicle stopping either before or after the traffic light.

To overcome this drawback, the current acceleration a_0 is here replaced with an average braking acceleration. The average braking acceleration $\tilde{a}$ is defined as:

$$\tilde{a} = -\frac{v_0^2}{2\,(D_{TL} - d_0^l)} \tag{9}$$

where D_{TL} represents the position of the traffic light , d_0^l represents the position and v_0 represents the velocity of the lead vehicle at $k = 0$. Note that this model formulation implies that the ego vehicle has access to V2I information, namely road grade, speed limits and location of stop signs and traffic signals within the N_H prediction horizon. Eq. (9) represents the minimum kinematic deceleration required by the lead vehicle to come to a stop at the traffic light. The modes of the CA-AB can be summarized as follows:

$$\hat{a}^l{}_k = \begin{cases} a_0, & \hat{v}_k^l < v_{lim}, \quad [FD] \\ 0, & \hat{v}_k^l \geq v_{lim} \vee \hat{v}_k^l = 0, \quad [FD] \\ \tilde{a}, & [S] \end{cases} \tag{10}$$

where FD and S stand for freeway driving and stop mode, respectively. The stop mode is activated in the presence of either a stop-sign or a traffic light with red signal phase within N_H .

Enhanced-Driver-Model with Line-of-Sight based Predictor (EDM-LOSP)

The existing EDM-LOS is a deterministic velocity predictor representing various levels of driver aggressiveness [4]. The EDM-LOS includes three distinct operating modes, namely, Car-Following (CF), Freeway Driving (FD) and Stop Mode (S). The different operating modes are represented by the following equations:

$$\hat{a}^l{}_k = \begin{cases} a\left(1 - \left(\frac{\hat{v}_k^l}{v_{lim} - \theta_0}\right)^{\delta}\right), \ v_0 \leq v_{lim} \quad [FD] \\ a\left(1 - \left(\frac{\hat{v}_k^l}{v_k^{l-1}}\right)^{\delta} - \left(\frac{s^*(\hat{v}^l, \Delta v)}{\Delta d_k^l}\right)^2\right), \quad [CF] \\ -\frac{1}{b}\left(\frac{(\hat{v}_k^l)^2}{2\Delta d_k^l}\right)^2, \quad [S] \end{cases} \tag{11}$$

$$\Delta d_k^l = d_k^{l-1} - d_k^l - d_{safe} \tag{12}$$

$$s_k^*(\hat{v}^l, \Delta v) = s_0 + \frac{\hat{v}_k^l \, (v_k^{l-1} - \hat{v}_k^l)}{2\sqrt{ab}} \tag{13}$$

$$s_{brake,k} = \left(1 + \frac{c_1}{\delta}\right)\left(\frac{\hat{v}^l{}_k^2}{2b}\right) \tag{14}$$

$\hat{v}_k^l$ and d_k^l represents the lead vehicle velocity and position, respectively. $[a, \delta, b, c_1, \theta_0]$ are the set of EDM-LOS calibration parameters. a represents the maximum acceleration and the exponent δ, representing driver aggressiveness, controls how quickly the desired speed is achieved. The freeway driving represents the transition to the route speed limit in the absence of any vehicle preceding the lead vehicle. The degree of aggressiveness is further characterized by a calibration term θ_0, which determines the offset from the route speed limit. As per this formulation, a relatively relaxed driver would drive slightly below the speed limit. The term b in the Stop mode represents the comfortable deceleration. When approaching an obstacle, such as a traffic light, the deceleration usually does not exceed b and is dynamically self-regulating towards a situation in which the kinematic deceleration equals b [3]. The driver aggressiveness on braking distance is captured by s_{brake}, which is dependent on a calibration term $\frac{c_1}{\delta}$. The Line-Of-Sight (LOS) scheme in the EDM is used to realistically model the drive response when approaching a traffic light. The LOS is a distance parameter below which, in presence of a traffic light, the driver can preview the signal phase of the upcoming traffic light. The presence of a traffic light at D_{TL} sets the flag TL = 1, when $D_{TL} - d_k^l \leq min\,(LOS, N_H)$. The driver performs a stop maneuver under two conditions, namely either if the previewed signal phase is red (SP = 3) or, the signal phase is yellow (SP = 8) and the vehicle is outside the critical braking zone s_{brake}. The term d_k^{l-1} in Δd_k^l is replaced by the position of the traffic light D_{TL} and s_{safe} set to zero. Therefore, stop mode is activated when:

$$\mathrm{S} = \begin{cases} 1, & TL = 1\,, SP = 3, d_k^l \leq LOS \\ 1, & TL = 1\,, SP = 8, s_{brake,k} < d_k^l \leq LOS \end{cases} \tag{15}$$

A detailed rule-based logic using LOS in the presence of a stop sign or traffic light is described in [16]. Regarding the car-following mode, d_k^{l-1} and v_k^{l-1} represent the position and speed of the vehicle preceding the lead vehicle. The absence of V2V communication makes this information unavailable for the ego vehicle to predict the car-following behavior, in particular deceleration events, of the lead vehicle. To overcome this, a modification of the freeway driving and stop mode equations is here developed (EDM-LOSP).

The prediction of the lead vehicle's transition to the desired speed in the FD mode uses only the current velocity, which is obtained by setting $\hat{v}_0^l = v_0$ in Eq. (11). Given availability of the current acceleration a_0 , it is possible to replace a with:

$$a_m = \frac{a_0}{1 - \left(\frac{v_0}{v_{lim} - \theta_0}\right)^{\delta}} \tag{16}$$

with $\hat{v}_0^l = v_0$, replacing a with a_m ensures that the first predicted acceleration $\hat{a}_0^l = a_0$. Ideally, this results into a perfect prediction for the first step, as in the case of a constant acceleration assumption. In addition, EDM-LOS is sensitive to the calibration parameters, in particular a and δ. When modelling driver behavior using EDM-LOS, these parameters are either calibrated offline from recorded driving data [17] or using online estimation techniques [18]. The sensitivity is also minimized by making use of the available current acceleration a_0. The other parameters δ and θ_0 remain calibratable, allowing one to capture different driver aggressiveness. The FD mode is employed when the current acceleration a_0 is non-negative. When a_0 is negative and there is no traffic light within N_H, the lead vehicle is assumed to brake because of the vehicle in front of the lead vehicle. Since the car-following mode in EDM-LOS cannot be employed, the stop mode is modified to predict the braking behavior. The comfortable deceleration b is replaced by the current acceleration a_0 and d_k^{l-1} term in Δd_k^l is replaced by assuming the lead vehicle is decelerating to a fixed obstacle at a position given by $\frac{v_0^2}{2|a_0|}$. One can observe that doing the above modifications to the stop mode results in converting to a constant acceleration model, as shown in appendix A.1. Incorporating the current acceleration a_0 of the lead vehicle, the equations of EDM-LOSP is summarized as:

$$\hat{a}^l{}_k = \begin{cases} a_m \left(1 - \left(\frac{\hat{v}_k^l}{v_{lim} - \theta_0}\right)^{\delta}\right), & v_0 \leq v_{lim}, a_0 \geq 0 \\ -\left(\frac{1}{a_0}\right)\left(\frac{\hat{v}_k^l}{2\left(\frac{v_0^2}{2|a_0|} - d_k^l\right)}\right), & a_0 < 0 \\ -\left(\frac{1}{b}\right)\left(\frac{\hat{v}_k^l}{2\left(D_{TL} - d_k^l\right)}\right), & S = 1 \end{cases} \tag{17}$$

Comparison of Predictor Performance

To highlight and compare the performance of the proposed predictors, a short driving profile was experimentally collected and used as

reference for the lead vehicle velocity. The speed prediction performance was quantified by computing the Root-Mean-Square-Error (RMSE) between the actual speed and the predicted speed. Prediction horizon lengths of 5, 10 and 15 seconds are evaluated for each predictor. The results are summarized in Table 1, showing the CA-AB and EDM-LOSP performing better over their counterparts. Fig.3 provides a visual description of how each velocity predictor performs (10 s prediction horizon) during a portion of the driving profile. The difference between CA and CA-AB can be mostly appreciated when the lead vehicle speed goes to zero in the presence of red phase traffic light (e.g., around 80 s). The CA does not predict the velocity to stop at the traffic light, as seen from the red lines close to 80s, indeed, a longer prediction horizon causes the velocity to pass the traffic light. The proposed CA-AB uses $\tilde{a}$ in the place of a_0 , hence predicting the lead vehicle stop at the traffic light. Summarizing, the advantages of using CA-AB over CA can be appreciated more in urban routes, due to the high traffic light and stops density. The portions of decreasing velocities of the lead vehicle, apart from the traffic light, for instance at ~10s, 25s and 50s are due the presence of vehicles preceding the lead vehicle. This behavior, given the availability of information on the vehicle preceding the lead, is predicted using the CF mode in EDM-LOS. However, without that information, this predictor assumes the lead vehicle to always be in FD mode predicting its velocity to reach a desired speed. The proposed EDM-LOSP overcomes this by identifying ($a_0 < 0$) and predicting decelerations using the second mode abovementioned in Eq. (17).

Table 1. RMSE in m/s of the different speed predictors for 5s, 10s and 15s future windows.

Prediction Horizon, s	CA	CA-AB	EDM-LOS	EDM-LOSP
5	1.00	0.97	1.80	0.81
10	2.63	2.40	2.70	2.24
15	3.67	3.45	3.47	3.15

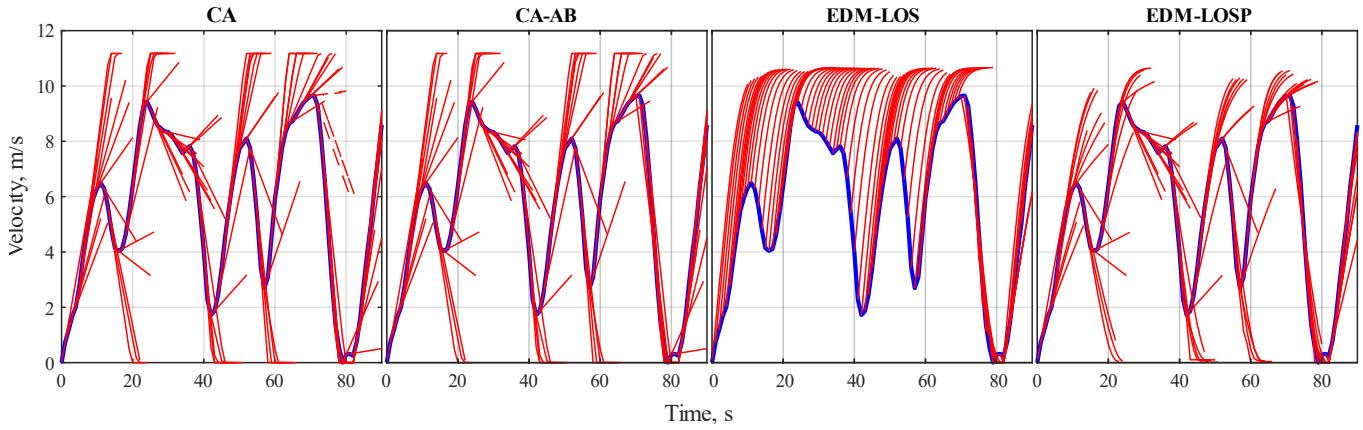

Figure 3. Speed predictions of the different for a 10 s prediciton window. In red, the velocities predicted at each timestep while in blue the actual lead vehicle speed.

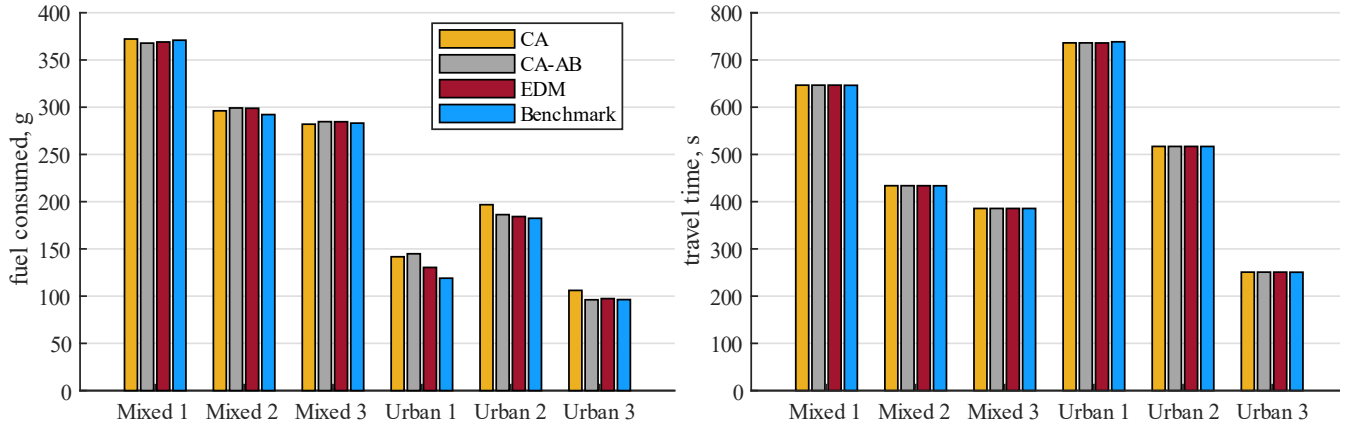

Figure 4. Bar plots for fuel consumed in grams (on the left) and travel time in seconds (on the right) for the six different routes and the different lead vehicle velocity predictors.

Simulation and Results

This section provides an application of the aforementioned lead vehicle velocity prediction methods. The performance of the proposed predictors, CA-AB and EDM-LOSP, are evaluated for energy efficiency and travel time using real-world driving profiles and compared against CA as baseline and an ideal scenario with perfect velocity prediction (wait-and-see) as benchmark. In general, information on future lead vehicle velocity is of crucial importance for the eco-driving optimal control problem, due to the knowledge needed to obtain the globally optimal solution. Absence of such information from V2V communication of any restriction of unavailability of data imply the need for reliable and robust algorithms to predict the future lead vehicle velocity trajectory. For conciseness, EDM-LOSP will be referred to as EDM for the rest of this section including figures.

For this analysis, different driving scenarios and routes were considered to demonstrate the utility of the speed predictors in the eco-driving problem. Six different routes were selected and divided between urban and mixed scenarios. The route data were obtained using GPS information extracted from different vehicles driven along the designated routes. It is worth mentioning that the location of traffic lights was known, however the Signal Phasing and Timing (SPaT) was not available, thus the need of defining a realistic SPaT by leveraging the time spent at stops by the lead vehicle. Additional information on the routes on traffic light density and average speed limits is provided in Table 2. For the sake of completeness, the speed limits, lead vehicle velocity and traffic light locations for the different routes are found in the Appendix (see Fig. A1), as a function of distance travelled.

Table 2. Routes information for urban and mixed driving scenarios.

Route name	Traffic light density, 1/km	Average speed limits, mph
Urban route 1	3.0	28
Urban route 2	1.2	40
Urban route 3	2.3	33
Mixed route 1	0.5	59
Mixed route 2	0.7	50
Mixed route 3	0.4	59

The results obtained using the rollout algorithm and the different speed predictors are shown in Fig. 4, in terms of total fuel consumed and travel time. As already mentioned, the optimization problem aims at minimizing both terms with an equal trade-off given as a weight in the cost function. It is worth noting that all the strategies implemented result charge sustaining, i.e., the initial and final SOC are approximately equal to 50%. The benchmark solution provided in these results corresponds to a perfect knowledge of the lead vehicle velocity in the prediction horizon (i.e., 200 m), and it is used to provide a fair and exhaustive comparison with the velocity predictors. From the bar plot in Fig. 4, it can be seen how the travel time remains practically unchanged among the different speed predictors, whereas the fuel consumed varies considerably. The highest differences are found in urban routes, where EDM and CA-AB consume an average of 3.9% and 7.9% more than the benchmark, respectively, while the CA leads to a fuel consumption increment of approximately 12.4%. In the mixed routes, no substantial changes are observed when applying the different predictors, mainly stemming from the higher portion of driving at constant speed where the different predictors act all similarly. The reasons why the EDM and corresponding eco-driving problem lead to an enhanced energy efficiency are worth analyzing in terms of Root-Mean-Square (RMS) of the acceleration. The CA speed predictor results in a higher RMS value for the acceleration in the urban routes with an average of 0.52 m/s^2, with respect to both CA-AB and EDM eco-driving approaches (i.e., 0.51 m/s^2 and 0.50 m/s^2 respectively). The higher value for acceleration RMS can be associated to higher fuel consumption, thus proving the differences just mentioned. An example of how the eco-driving solution approaches the traffic lights is shown in Fig. 5 and mostly visible in the zoomed window that highlights two close traffic lights. It can be noticed how the prediction of lead vehicle speed along with the signal phase knowledge allows the ego vehicle to not stop at traffic lights when it is feasible, thus avoiding inefficient deceleration to null speed and subsequent acceleration. Analyzing further the zoomed window, it can be seen that the benchmark solution starts decelerating long before the first traffic light and accelerates only towards the end of the green phase, just enough to avoid stopping. Further differences can be seen also in the behavior of the CA eco-driving approach (in yellow in Fig. 5) that accelerates right after the lead vehicle leaves the traffic light and then decelerates when the gap is low.

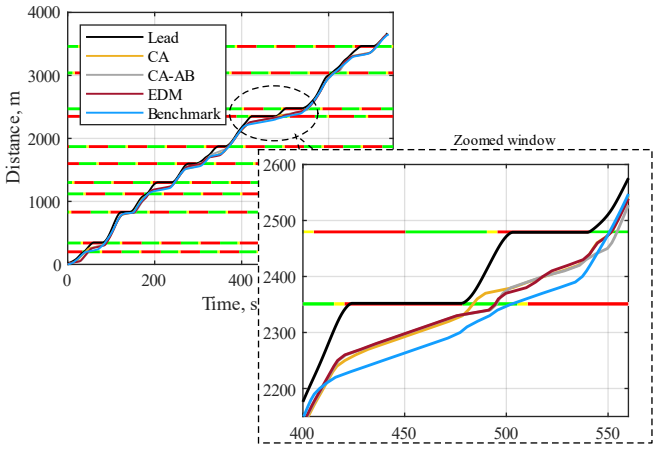

Figure 5. Traffic lights SPaT and trajectories of the lead vehicle and the different eco-driving approach using the diverse velocity predictors.

For the sake of completeness, Fig. 6 illustrates the eco-driving solutions with the different speed predictors implemented on Mixed Route 2. In general, no visible differences are found among the different predictors' solutions. However, all demonstrate smoother velocities with respect to the lead vehicle avoiding unnecessary slowdowns (see Fig. 6 around 840 m and 2815 m), thus improving overall energy efficiency.

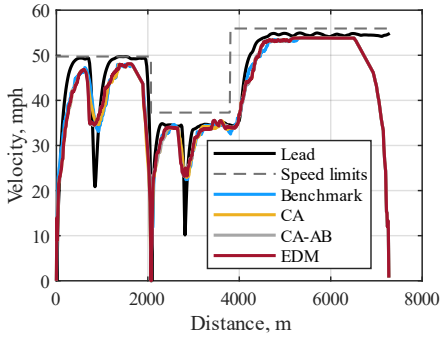

Figure 6. Velocity traces for the different speed predictors and eco-driving problems in Mixed Route 2, as a function of distance.

The reason why the travel time does not vary as noticeably as the fuel consumption is attributable to the need of complying with traffic lights phases and the impossibility of passing the lead vehicle. To confirm this statement, two other rollout algorithms have been run with different weights between fuel consumed and travel time (i.e., γ introduced in previous section). Even when orienting the cost function to penalize more the travel time than the fuel consumption, no substantial variations are found, as seen in Fig. 7 below concerning simulations on Urban route 1. It is worth noting that the y-axis in Fig. 7 is magnified for the sake of clarity and that the differences between the neutral cost function and the one mostly oriented towards travel time (i.e., $\gamma = 0.5$ and $\gamma = 0.2$, respectively) are in the orders of seconds, hence confirming that the constraints posed by the lead vehicle and the traffic lights do not allow room for variation, as mentioned above.

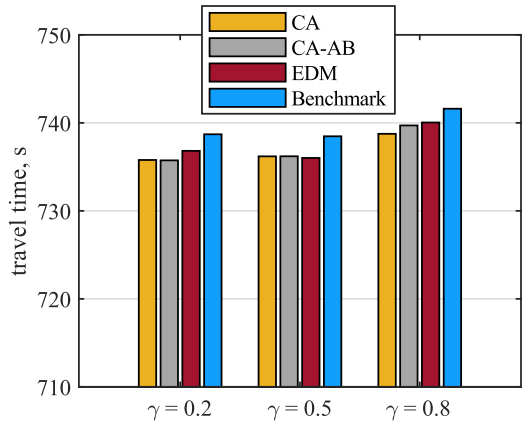

Figure 7. Bar plots graph of the travel times obtained using different speed predictors and different weights in the DP cost function in Urban Route 1.

Conclusions

The lead vehicle velocity prediction improves with the availability of the V2V information about the vehicles preceding the lead vehicle. However, in the absence of V2V communication or in data-restricted environment, the prediction accuracy reduces. To mitigate this, two predictors, namely CA-AB and EDM-LOSP, were developed to predict lead vehicle velocity without the need of V2V communication. First, a CA predictor was modified to incorporate an average deceleration part while slowing down or stopping. Second, the EDM-LOS was modified to incorporate current acceleration information in capturing lead vehicle decelerations during car-following. A comparative study was conducted to analyze the prediction accuracy of the developed predictors over different prediction horizons. A time-gap based constraint was designed leveraging the predicted lead vehicle velocity over the prediction horizon. This information was then integrated into a non-linear eco-driving optimal control problem. Large scale simulations were performed over 6 real-world routes representing urban and mixed driving scenarios to solve the eco-driving problem as a MPC with the developed predictors. Results show higher energy savings considering the EDM-LOSP for urban driving with respect to the CA and CA-AB. This confirms the importance of accurate predictions of preceding traffic to enhance energy efficiency, especially in urban scenarios. Future work will include testing the eco-driving controller embedding the information coming from the EDM-LOSP using hardware-in-the-loop simulation.

References

1. Jacome, O., Gupta, S., Stockar, S., and Canova, M. "Data-driven Driver Model for Speed Advisory Systems in Partially Automated Vehicles." *arXiv preprint arXiv:2205.08445* (2022).
2. Kamal, M. A. S., Masakazu, M., Junichi, M., and Taketoshi, K. "Ecological driving based on preceding vehicle prediction using MPC." *IFAC Proceedings Volumes* 44, no. 1 (2011): 3843-3848.
3. Lakshmanan, V. K., Sciarretta, A., and El Ganaoui-Mourlan, O. "Cooperative Eco-Driving of Electric Vehicle Platoons for Energy Efficiency and String Stability." *IFAC-PapersOnLine* 54, no. 2 (2021): 133-139.
4. Sciarretta, A., and Ardalan, V. "Energy saving potentials of CAVs." In *Energy-Efficient Driving of Road Vehicles*, pp. 1-31. Springer, Cham, 2020.
5. Bhagdikar, P., Gankov, S., Rengarajan, S., Sarlashkar, J., Hotz, S., & Bakshi, K. "Quantifying System Level Impact of Connected and Automated Vehicles in an Urban Corridor," (No. 2022-01-0153). SAE Technical Paper, 2022.
6. Hyeon, E., Kim, Y., Prakash, N., and Stefanopoulou, A.G. "Influence of Speed Forecasting on the Performance of Ecological Adaptive Cruise Control," in *Dynamic Systems and Control Conference*, Utah, 2019.
7. Asher, Z. D., Baker, D. A., and Bradley, T. H., "Prediction Error Applied to Hybrid Electric Vehicle Optimal Fuel Economy," *IEEE Transactions on Control Systems Technology*, pp. vol. 26, no. 6, pp. 2121-2134, 2018.
8. Hyeon, E., Speed Forecasting Strategies for the Energy-Optimal Car-Following of Connected and Automated Vehicles. Michigan: Doctoral Thesis, 2022.
9. Treiber, M. and Krestig, A., "Car-Following Models Based on Driving Strategies," in *Traffic Flow Dynamics: Data, Models and Simulation*. Berlin,Heidelberg: Springer Berlin Heidelberg, 2013, pp. 181-204.
10. Gupta, S., Deshpande S.R., Tulpule, P., Canova, M., and Rizzoni, G., "An Enhanced Driver Model for Evaluating Fuel Economy on Real-World Routes," in *Advances in Automotive Control* , Orleans, 2019, pp. Pages 574-579.
11. Brackstone, M. and McDonald, M., "Car-following: a historical review," *Transportation Research Part F: Traffic Psychology and Behaviour*, vol. 2, no. 4, pp. 181-196, Decemeber 1999.
12. Li, Y., Mingnuo, C., and Wanzhong, Z. "Investigating long-term vehicle speed prediction based on BP-LSTM algorithms." *IET Intelligent Transport Systems* 13, no. 8 (2019): 1281-1290.
13. Gupta, S., and Canova, M. "Eco-Driving of Connected and Autonomous Vehicles with Sequence-to-Sequence Prediction of Target Vehicle Velocity," in *IFAC*, Tokyo, Japan, 2021, pp. Volume 54, Issue 10, Pages 430-436.
14. Deshpande, S.R., Gupta, S., Gupta, A., and Canova, M. "Real-Time Eco driving Control in Electrified Connected and Autonomous Vehicles Using Approximate Dynamic Programing." *Journal of Dynamic Systems, Measurement, and Control* 144, no. 1 (2022): 011111.
15. Zhu, Z., Gupta, S., Pivaro, N., Deshpande, S.R., and Canova, M. "A gpu implementation of a look-ahead optimal controller for eco-driving based on dynamic programming." In *2021 European Control Conference (ECC)*, pp. 899-904. IEEE, 2021.
16. Deshpande, S.R., Gupta, S., Kibalama, D., Pivaro, N., and Canova, M. "Benchmarking fuel economy of connected and automated vehicles in real world driving conditions via monte carlo simulation," in *ASME Dynamic Systems and Control Conference*, Pittsburgh,PA, 2020.

17. Hegde, B., O'Keefe, M., Muldoon, S., Gonder, J., and Change C. "Real-World Driving Features for Identifying Intelligent Driver Model: Preprint.," in *SAE WCX World Congress Experience Digital Summit*, 2021, pp. NREL/CP-5400-78817.
18. Monteil, J., O'Hara, N., Cahill, V., and Bouroche, M. "Real-time estimation of drivers' behaviour," in *International Conference on Intelligent Transportation Systems*, 2015.

Contact Information

Vinith Kumar Lakshmanan, vinith-kumar.lakshmanan@ifp.fr

Appendix

A.1: Proof of stop mode in EDM-LOSP is equivalent to CA

Following, a proof is given that the stop mode in EDM-LOSP is equivalent to a constant acceleration prediction. The proof is given for the predictor equations in continuous time, but the same result holds for the discrete system.
Given the current instantaneous speed v_0 and acceleration a_0, let $s^l(t), v^l(t)$, be the lead vehicle position and speed, respectively, where:

$$\frac{ds^l}{dt} = v^l(t), \qquad s^l(0) = 0 \tag{A1}$$

The stop mode in the EDM-LOSP is then given by:

$$\hat{a}(t) = \frac{dv^l}{dt} = -\frac{1}{|a_0|}\left(\frac{v^l(t)^2}{2\Delta x(t)}\right)^2 = -\frac{a_{kin}^2(t)}{|a_0|} = -a_{kin}(t)\left(\frac{a_{kin}(t)}{|a_0|}\right), \qquad v^l(0) = v_0, \tag{A2}$$

where $\Delta x(t)$ is the distance of the lead vehicle from the next predicted stop.

Theorem 1:
If $\Delta x(t) \coloneqq \frac{v_0^2}{2|a_0|} - s^l(t)$, *then* $a^l(t) = -|a_0|$

Proof:
The proof proceeds by showing that:

1. $a_{kin}(t) = |a_0|$, is an equilibrium point for the acceleration.
2. By the definition of $\Delta x(t)$, the equilibrium is attained at $t = 0$ and $\hat{a}(t) = -|a_0|$

Let $a_{kin}(t) = \frac{v^l(t)^2}{2\Delta x(t)}$, then:

$$\frac{\mathrm{da_{kin}}}{\mathrm{dt}} = \frac{4\mathrm{v^l(t)}\frac{\mathrm{dv^l}}{\mathrm{dt}}\Delta\mathrm{x(t)} - 2\mathrm{v^l(t)^2}\frac{\mathrm{d}\Delta\mathrm{x}}{\mathrm{dt}}}{4\Delta\mathrm{x(t)^2}} = \frac{\mathrm{v^l(t)}}{\Delta\mathrm{x(t)}}\left(\frac{\mathrm{a_{kin}(t)}}{|\mathrm{a_0}|}\right)(|\mathrm{a_0}| - \mathrm{a_{kin}(t)}). \tag{A3}$$

Hence $a_{kin}(0) = |a_0|$ entails that a_{kin} remains constant.
Now, from the definition of Δx it follows $\Delta x(0) = \frac{v_0^2}{2|a_0|}$. By substitution in the expression for a_{kin} and recalling the initial condition on v^l it can be shown:

$$a_{kin}(0) = \frac{v^l(0)^2}{2\Delta x(0)} = \frac{v_0^2}{2(\frac{v_0^2}{2|a_0|})} = |a_0| \quad \rightarrow \quad \hat{a}(t) = \frac{dv^l}{dt} = -\frac{a_{kin}(t)^2}{|a_0|} = -|a_0| \tag{A4}$$

A.2: The urban and mixed routes with lead vehicle velocity and routes features

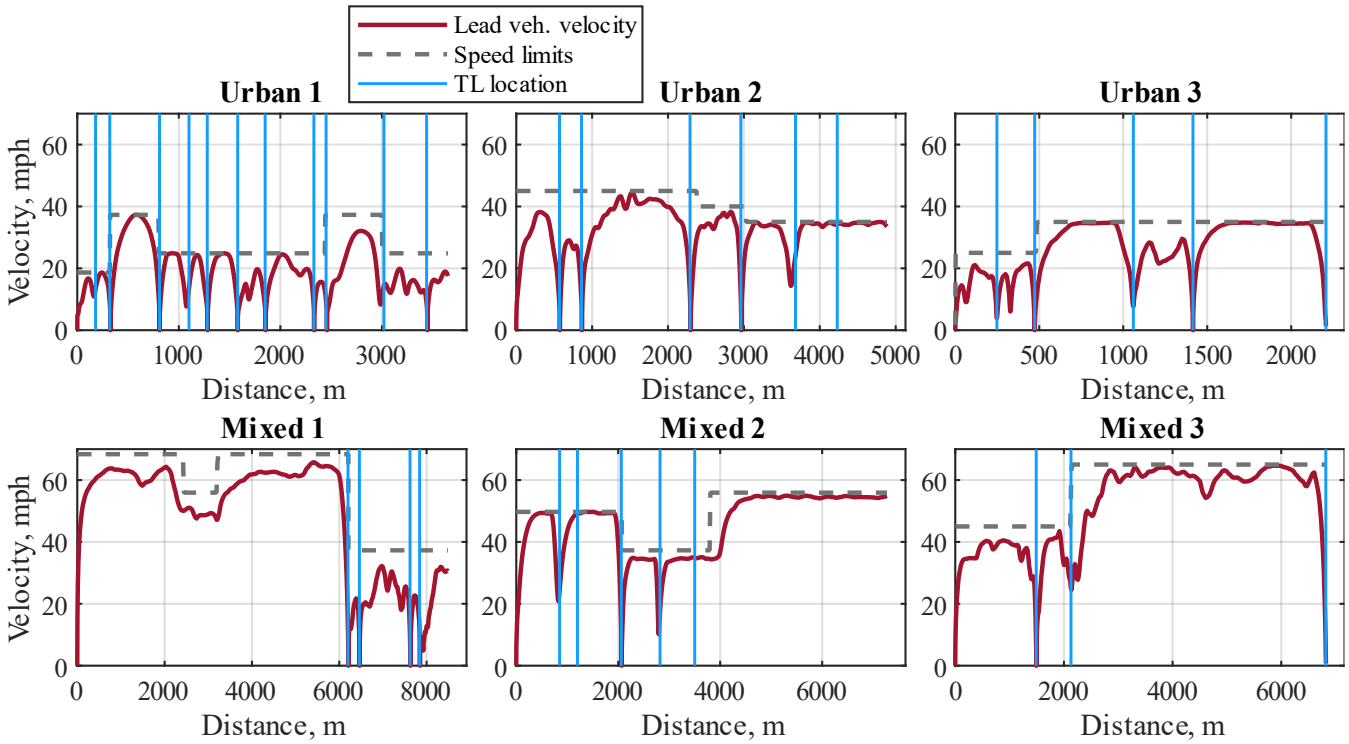

Figure A1. Speed limits, traffic lights locations and lead vehicle velocity profiles for the six different urban and mixed routes, as a function of the distance.